Noninvasive optoacoustic online retinal temperature determination during continuous-wave laser irradiation

Jochen Kandulla
Universität zu Lübeck
Institut für Biomedizinische Optik
Peter-Monnik-Weg 4
D-23562 Lübeck, Germany
E-mail: kandulla@bmo.uni-luebeck.de

Hanno Elsner
Universitätsklinikum Schleswig Holstein Campus Kiel
Klinik für Augenheilkunde
Hegewischstrass 2
24105 Kiel, Germany

Reginald Birngruber
Ralf Brinkmann
Universität zu Lübeck
Institut für Biomedizinische Optik
Peter-Monnik-Weg 4
D-23562 Lübeck, Germany

Abstract. The therapeutic effect of most retinal laser treatments is initiated by a transient temperature increase. Although crucial to the effectiveness of the treatment, the temperature course is not exactly known due to individually different tissue properties. We develop an optoacoustic method to determine the retinal temperature increase in real time during continuous-wave (cw) laser irradiation, and perform temperature calculations to interpret the results exemplary for transpupillary thermotherapy (TTT). Porcine globes *ex vivo* and rabbit eyes *in vivo* are irradiated with a diode laser ($\lambda = 810$ nm, $P \leqslant 3$ W, $\phi = 2$ mm) for 60 s. Simultaneously, pulses from a N_2-laser pumped dye laser ($\lambda = 500$ nm, $\tau = 3.5$ ns, $E \approx 5$ μJ) are applied on the retina. Following its absorption, an ultrasonic pressure wave is emitted, which is detected by a transducer embedded in a contact lens. Using the previously measured temperature-dependent Grüneisen coefficient of chorioretinal tissue, a temperature raise in porcine eyes of 5.8 °C/(W/cm^2) after 60 s is observed and confirmed by simultaneous measurements with an inserted thermocouple. In a rabbit, we find 1.4 °C/(W/cm^2) with, and 2.2 °C/(W/cm^2) without perfusion at the same location. Coagulation of the rabbit's retina occurs at $\Delta T = 21$ °C after 40 s. In conclusion, this optoacoustic method seems feasible for an *in vivo* real-time determination of temperature, opening the possibility for feedback control retinal laser treatments.
 [DOI: 10.1117/1.2236301]

Keywords: temperature; optoacoustics; transpupillary thermotherapy; ultrasonic transducer; laser; heat diffusion calculations; retinal laser treatment.

Paper 05282SSRR received Sep. 30, 2005; revised manuscript received Jan. 23, 2006; accepted for publication Jan. 23, 2006; published online Aug. 23, 2006.

1 Introduction

The most common field of medical laser application is ophthalmology. Therapies include classical photocoagulation,[1] photo dynamic therapy (PDT),[2] selective retina treatment (SRT),[3] and transpupillary thermotherapy (TTT).[4–6] In most of these applications, the therapeutic effect results from a retinal temperature increase. As the temperature increase is highly influenced by individual tissue properties, like light absorption in retinal pigment epithelium (RPE) and choroid, choroidal blood flow, and light scattering of the anterior ocular media, it can only be estimated by assuming average values of the tissue properties. Hence, it is desirable to establish a noninvasive dosimetry control based on a real-time retinal temperature determination during the previously mentioned laser treatments.

A good example for a long exposure time treatment is transpupillary thermotherapy (TTT), which treats occult subfoveal choroidal neovascularizations (CNVs) secondary to age-related macula degeneration (ARMD). In TTT, diode laser irradiation with a wavelength of 810 nm is used to thermally treat the diseased area. Typically 800 mW, incident on the cornea, a retinal spot diameter of 3 mm, and an irradiation time of 60 s are used.[7] The absorption of the laser radiation at the fundus of the eye causes a chorioretinal temperature increase, which ideally evokes endothelial damage of the CNV with subsequent thrombosis and regression of the new vessels. This potentially could stabilize or even improve visual acuity.[8] However, under the same laser parameters, the individual temperature increase might result in undertreatment or even overtreatment with a coagulation of the photoreceptors, causing severe visual loss.[9] If an optimum treatment temperature exists, it could be reproducibly realized by automatically adjusting the TTT laser power individually to achieve said optimal treatment temperature below the coagulation threshold. This could significantly improve safety and efficacy of TTT and other thermal laser treatments.

Temperature increase of biological tissue was first optoacoustically determined during heating and cooling of canine liver.[10–12] In ophthalmology, this technique was attempted

Address all correspondence to Jochen Kandulla, Institut für Biomedizinische Optik, Universität zu Lübeck, Peter-Monnik-Weg 4, Lübeck, S-H 23552 Germany; Tel: +49–451–5006517; Fax: +49–451–5006546; E-mail: kandulla@bmo.uni-luebeck.de

1083-3668/2006/11(4)/041111/13/$22.00 © 2006 SPIE

with microsecond laser pulses *in vitro* on porcine RPE explants,[13] as well as on patients undergoing SRT.[14] *Ex vivo* results on porcine globes showed that such optoacoustic (OA) techniques also allow for chorioretinal temperature determination during TTT.[15]

The objective of this study is to quantify the measurement accuracy of OA temperature determination during retinal cw-laser irradiation. The influence on choroidal perfusion to the chorioretinal temperature increase is examined, and the temperature threshold for coagulation is quantified.

The obtained experimental data are compared with analytical calculations utilizing a model based on two absorbing layers at the fundus of a rabbit eye.[16,17] This model is also used for a general discussion of the influence of tissue parameters on the chorioretinal temperature profile.

2 Materials and Methods

2.1 *Theoretical Background of Pressure Generation*

If an absorber is irradiated with laser pulses, the light absorption leads to heating and a subsequent thermoelastic pressure generation. The pressure is dependent on the absorption coefficient α, radiant exposure H, absorber depth z, and the temperature-dependent Grüneisen parameter Γ of the material [Eq. (1)]. Neglecting the temporary temperature rise caused by the absorption of the laser pulse and considering conditions of stress confinement, a spot with a diameter larger than the absorption depth and uniform irradiance across the laser beam, the pressure induced in the absorber is:[18–20]

$$p_0(z,T) = \alpha H \Gamma(T) \exp(-\alpha z), \tag{1}$$

with

$$H = \frac{E}{A}, \tag{2}$$

where E=pulse energy and A=irradiated area.

The induced pressure causes thermoelastic expansion of the tissue and the emission of a pressure wave. The maximum amplitude of this pressure wave at some distance is directly proportional to pulse energy and the Grüneisen parameter Γ:[21]

$$p_{\max}(T) \sim H\Gamma(T) \sim E\Gamma(T). \tag{3}$$

The dimensionless Grüneisen coefficient Γ relates the initial pressure to the absorbed volumetric energy density. It is material specific and depends on the volumetric expansion coefficient β, the speed of sound c_0, and the specific heat capacity c_p of the material:

$$\Gamma(T) = \frac{\beta(T) c_0^2(T)}{c_p(T)}. \tag{4}$$

All parameters are temperature dependent. However, the influence of c_0 and c_p is negligible compared to that of β, e.g., for water between 37 °C and 50 °C, the value for β increases by 26.46%, whereas the values of c_0 and c_p increase only by 1.24 and 0.05%, respectively.[22] The temperature dependence of the Grüneisen parameter is known for water up to temperatures in the metastable state around 300 °C.[23] In the range of 0 to 100 °C, it can be approximated by a second-order polynomial:[19]

$$\Gamma(T) = a_1 T^2 + a_2 T + a_3. \tag{5}$$

By conversion this equation can be written in the following form:

$$\Gamma(T) = a_1[(T^2 - T_0^2) - 2T_{\max}(T - T_0)], \tag{6}$$

with $T_{\max} = -a_2/2a_1$ and $T_0 = -a_2/2a_1 - (a_2^2/4a_1^2 - a_3/a_1)^{1/2}$. In this form, the polynomial coefficients a_2 and a_3 are characterized by the parameters T_0 and $T_{\max}$. T_0 indicates the temperature for which $\beta(T)$ and therefore $\Gamma(T)=0$, and $T_{\max}$ is the temperature for which $\Gamma(T=T_{\max})$ reaches the maximum. For water, T_0 is 3.98 °C at its state of maximum density. For the absorbing media of the fundus of the eye, T_0 and $T_{\max}$ act as useful fitting parameters and have to be determined experimentally. This can be done by detection of $p_{\max}$ at different temperatures of the fundus and approximation of a second-order polynomial with fitting parameters T_0 and $T_{\max}$.

With the approximation of a polynomial relation between Γ and temperature T, the maximum pressure amplitude as given in Eq. (3) results in:

$$p_{\max}(T) = sE[(T^2 - T_0^2) - 2T_{\max}(T - T_0)]. \tag{7}$$

In this relation, s is a proportionality factor that is unique for every irradiation spot. It takes into account not only the polynomial coefficient a_1 [Eq. (6)], absorption coefficient α, and the irradiated area A [Eq. (1)], but also the acoustic transfer function from the source to the detector, transducer characteristics, and signal amplification.

2.2 *Temperature Determination from Pressure Signal*

If the material constants T_0 and $T_{\max}$ are known for the chorio-retinal tissue, a temperature increase can be determined from the maximum amplitude of the laser-induced pressure wave according to Eq. (7). For this purpose the individually varied proportionality factor s has to be determined once before each measurement. This can be performed by applying probe pulses with the known energy E, detecting $p_{\max}$ at a known temperature $T=T_{\text{ref}}$ of the absorbing media, and conversion of Eq. (7). For *in vivo* temperature determination, T_{ref} is the body temperature.

With the knowledge of s, all parameters of Eq. (7) are defined, and the temperature increase during laser-induced tissue heating can thereafter be calculated from $p_{\max}$ according to Eq. (8):

$$T(p_{\max}) = T_{\max} - \left[T_{\max}^2 + \frac{p_{\max}(T)}{sE} + T_0^2 - 2T_{\max}T_0 \right]^{1/2}. \tag{8}$$

Pulse-to-pulse fluctuations of the probe laser are taken into account by normalizing the maximum pressure $p_{\max}(T)$ to the laser pulse energy E.

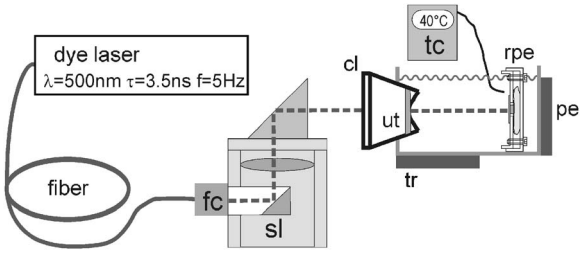

Fig. 1 Experimental setup for a determination of the temperature dependence of the Grüneisen parameter. sl: slit lamp; fc: fiber coupler; cl: contact lens; ut: ultrasonic transducer; rpe: RPE explant; tc: thermocouple; tr: thermal resistor; and pe: peltier element.

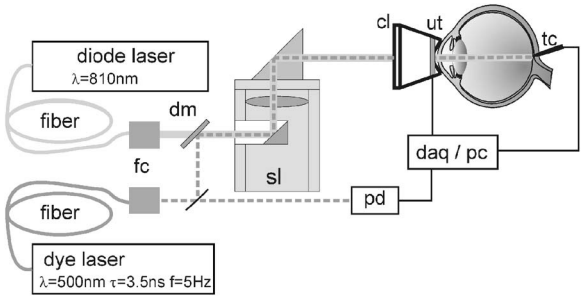

Fig. 2 Experimental setup for chorioretinal temperature determination by OA. fc: fiber coupler; pd: photodiode; dm: dichroic mirror; sl: slitlamp; cl: contact lens; ut: ultrasonic transducer; tc: thermocouple; daq: data acquisition; and pc: personal computer.

2.3 *Experimental Setup for Determination of T_0 and T_{max}*

The *ex vivo* calibration experiments on porcine and rabbit retinal explants to determine T_0 and T_{max} were carried out within four hours postmortem. First, the macula was dissected from the eye. Then the vitreous body and neural retina were carefully removed. To prevent drying, the retinal explant was covered with physiological saline solution.

Laser pulses of a nitrogen laser pumped dye laser (LSI Laser Science, VSL337ND with Coumarin500, $\lambda = 500$ nm, $E \approx 5$ μJ $\tau = 3.5$ ns, $f = 5$ Hz) were coupled to an optical fiber (Ceram Optec, 50 μm, NA=0.11), which was directly connected to a slit lamp (*sl*, Zeiss, 30 SL/L). The tip of the fiber was imaged through an ophthalmic contact lens (*cl*, Mainster Standard or Haag-Streit 903) onto the surface of a retinal explant. By the slit lamp magnification, the laser spot diameter on the surface could be adjusted between 50 μm and 1 mm with a spatial top-hat beam profile. Assuming a pulse energy of 5 μJ and a spot diameter of 0.3 mm, the light absorption in the RPE [$\alpha = 1700$ cm^{-1} (Ref. 24)] causes a temporary maximal temperature increase of less than 3 °C. The average power for a repetition rate of 5 Hz is 25 μW, which induces a negligible baseline temperature of <50 mK.

The retinal explant was positioned in a cuvette filled with physiological saline solution. The laser-induced pressure wave propagated through the water bath and was detected by a ring-shaped ultrasonic transducer (*ut*, lead zirconium titanate, PZT5) embedded in the contact lens (Fig. 1). By means of a thermal resistor (*tr*) and peltier elements (*pe*), the ambient temperature of the saline solution and, consequently, of the retinal explant could be regulated in the range of 5 to 60 °C. The current temperature of the water bath was measured by a thermocouple (*tc*) positioned close to the retinal explant. A magnetic stirrer (Hanna, HI190M) was used to move the saline solution to prevent ambient temperature gradients within the water bath.

2.4 *Experimental Setup for Optoacoustic Temperature Determination*

The *ex vivo* experiments on OA temperature determination were performed on whole porcine eyes within four hours postmortem with the contact lens directly positioned on the cornea.

The *in vivo* experiments two on rabbits were carried out under ethical guidelines for animal treatment with permission of the ethical committee of the University of Kiel.

The rabbit was anesthetized right before the measurement by a mixture of xylacinehydrochloride and ketaminehydrochloride. It was then placed in a special holding device and positioned in front of the slit lamp. The rabbit's cornea was additionally anesthetized with xylocaine eye drops, and the pupils were dilated with neosynephrine eye drops. The contact lens with the integrated ultrasonic transducer was fixed on the rabbit's cornea and kept stable during the measurement. For a better acoustic adaption to the ultrasonic transducer, some drops of Methocel® were used as a contact gel.

To determine the chorioretinal temperature increase during laser heating, an experimental setup as shown in Fig. 2 was used. The fiber-coupled pulsed dye laser was connected to a slit lamp (*sl*, Zeiss, Visulas Argon). Additionally, the radiation of a TTT laser (CeramOptec, $\lambda = 810$ nm, $P \leqslant 3$ W) was coupled via a fiber concentrically into the same optical path as the probe laser radiation utilizing a dichroic mirror (*dm*). The two fiber tips were imaged onto the fundus of the eye using a retinal top-hat beam profile with independently adjustable spot diameters between 50 μm to 1 mm (probe laser spot) and 0.5 to 5.5 mm (TTT laser spot). The energy of the dye laser was measured by a photodiode (*pd*, FND100). As in the previous setup, the ultrasonic pressure wave was detected by a ring transducer integrated into the contact lens. To verify the OA-determined temperature increase, a miniaturized thermocouple (*tc*, Rössel Messtechnik, type K, diameter 250 μm) was positioned through the sclera below the RPE layer into the center of the TTT laser spot. For *in vivo* measurements on rabbit eyes, the thermocouple was inserted through a sclerotomy into the center of the irradiation spot. All data were acquired (*daq*) and analyzed by a personal computer (PC).

2.5 *Data Acquisition*

For an online monitoring of laser-induced temperature increase, all data acquisition and analysis need to be performed in real time. The signal of the ultrasonic transducer is amplified by a preamplifier (Panametrics 5662) by 54 dB and digitized by an 8-bit high-speed digitizer (National Instruments, NI 5112, 100 MHz, two channel). The second channel is used for the pulse energy signal from the photodiode and as a trig-

ger signal. The temperature measurement is achieved by a thermocouple input board (Measurement Computing PCI-DAS-TC).

The real-time signal processing and display was programmed in LabView® 6.0i software. To increase the signal-to-noise ratio, the ultrasonic transients underwent a software-based frequency filtering (Butterworth fourth order, bandpass 50 kHz to 3 MHz). The maximum amplitude of the first peak was recorded as $p_{\max}$. The obtained temperature curves were filtered utilizing a fifth-order median filter.

2.6 *Analytical Modeling of Heat Diffusion*

In order to compare the experimentally obtained data with temperature simulations, we used an analytical model based on two absorbing layers, assuming homogeneous and isotropic heat conduction and negligible light scattering. The changes in temperature that occur from laser exposure are described by the heat diffusion equation:

$$\frac{\partial T}{\partial t} - \kappa \Delta T = \frac{\varepsilon}{\rho c_p}, \tag{9}$$

where ε represents the externally added energy per unit volume and time.[16,25]

Due to heat convection arising from blood circulation in the choroid, a global perfusion term is added to the source term ε. This can be achieved by assuming the subtraction of a quantity of heat with a constant rate Q within the whole volume. Therefore, the perfusion term $\rho c_p Q T$, acting as a heat sink, is subtracted from the source term ε.[17,26] As the blood circulation and hence the perfusion is physiologically localized in the choroid, the assumption of a global heat sink is an overestimation, resulting in lower perfusion rates.

$$\frac{\partial T}{\partial t} - \kappa \Delta T = \frac{\varepsilon}{\rho c_p} - QT. \tag{10}$$

The solution of Eq. (10) is given by[26]

$$T(\vec{r},t) = \int_0^t dt' \int_{-\infty}^{+\infty} dr' G(\vec{r},\vec{r}',t,t') \varepsilon(\vec{r}',t) \exp(-Qt'), \tag{11}$$

where

$$G(\vec{r},\vec{r}',t,t') = \frac{\theta(t-t')\exp[-|r-r'|/4\kappa(t-t')]}{8\rho c_p[\pi\kappa(t-t')]^{3/2}} \tag{12}$$

is the infinite domain Green function and θ is the Heaviside function.

The source term ε is dependent on the beam profile of the laser spot. With respect to the experimental setup, we assumed a top-hat laser profile in time and space. For the analytical modeling, we approximated a square laser beam profile (side length, $2a$) covering the same area as the circular beam spot with radius r, thus $2a = r\sqrt{\pi}$.

The fluence rate $I(x,y,z)$ in the tissue, assuming one absorbing layer of the thickness d for the top-hat laser spot, is given by the Lambert-Beer law:

$$I(x,y,z) = \begin{cases} I_0 & \text{for } 0 \leq |x| \leq a, 0 \leq |y| \leq a \text{ and } z < 0 \\ I_0 e^{-\alpha z} & \text{for } 0 \leq |x| \leq a, 0 \leq |y| \leq a \text{ and } 0 \leq z \leq d \\ I_0 e^{-\alpha d} & \text{for } 0 \leq |x| \leq a, 0 \leq |y| \leq a \text{ and } z > d \end{cases}. \tag{13}$$

The energy per volume and unit of time deposited in the irradiated tissue is the negative derivative of Eq. (13) and can be calculated to:[25,26]

$$\varepsilon(x,y,z,t) = \begin{cases} \alpha I_0 \exp(-\alpha z) & \text{for } 0 \leq |x| \leq a, \\ & 0 \leq |y| \leq a, \\ & 0 \leq z \leq d, \\ & \text{and } 0 \leq t \leq \tau \\ 0 & \text{otherwise} \end{cases}, \tag{14}$$

with τ=exposure time.

With the described approximations, Eq. (11) can be solved analytically using the source term of Eq. (14):[27,28]

$$\begin{aligned} T(\vec{r},t) = \frac{\alpha I_0}{8\rho c_p} \int_0^t dt' \, \theta(\tau + t' - t) \exp(-\alpha z + \alpha^2 \kappa t' - Qt') \\ \times \left[\operatorname{erf}\left(\frac{x-a}{2\sqrt{\kappa t'}} \right) - \operatorname{erf}\left(\frac{x+a}{2\sqrt{\kappa t'}} \right) \right] \\ \times \left[\operatorname{erf}\left(\frac{y-a}{2\sqrt{\kappa t'}} \right) - \operatorname{erf}\left(\frac{y+a}{2\sqrt{\kappa t'}} \right) \right] \\ \times \left[\operatorname{erf}\left(\frac{z}{2\sqrt{\kappa t'}} - \alpha\sqrt{\kappa t'} \right) - \operatorname{erf}\left(\frac{z-d}{2\sqrt{\kappa t'}} - \alpha\sqrt{\kappa t'} \right) \right]. \end{aligned} \tag{15}$$

This equation gives the spatial and temporal temperature increase induced by the absorption of laser light with a top-hat beam profile in space and time in a single layer under the assumption of an infinite layer in lateral direction.

2.7 *Layer Structure at the Fundus*

For temperature calculations, a rabbit eye model consisting of two absorbing layers was used: the retinal pigment epithelium (RPE) and the choroid. The absorption for human RPE was reported in the range from 400- to 1100-nm wavelength.[31] These data were used to calculate the spectral absorption coefficient for human RPE by assuming an absorber thickness of 10 μm. For rabbit RPE and choroid the absorption is known from 400- to 700-nm wavelength.[29,30] According to the rabbit eye geometry published by Birngruber[17] the rabbit RPE has a thickness of 4 μm and the pigmented choroid of 20 μm. The rabbit absorption coefficients for the irradiation wavelength of 810 nm were derived by extrapolating the absorption data and assuming a constant ratio of absorption coefficient for human RPE to rabbit RPE respective choroid. The ratio was derived for $\lambda = 650$ nm. The corresponding curves are depicted in Fig. 3. Under these assumptions a fundus geometry as shown in Fig. 4 was used for the temperature simulations. The RPE had a thickness of 4 μm, resulting in an absorption coefficient of 169 cm^{-1} for a wavelength of 810 nm. The adjacent choroid

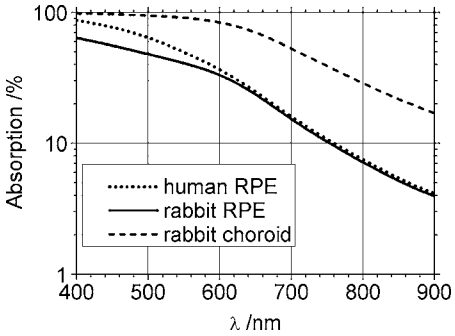

Fig. 3 Absorption of human RPE, rabbit RPE, and rabbit choroid as a function of wavelength derived from Refs. 29–31.

was 61 μm thick with melanin concentrated in the posterior third of the choroid, thus, an absorption coefficient of 156 cm^{-1}. The sclera was assumed to scatter the remaining light out of the regarded volume without absorption. Due to absorption and scattering in the anterior part of the eye including lens and vitreous, only 90% of the power incident at the cornea was assumed to reach the fundus of the rabbit eye.[32–35]

As biological tissue consists mainly of water, the material specific parameters $\rho=0.993\ g/cm^3$ (density), $c_p=4.179\ J/(g\,K)$ (specific heat capacity), and $\kappa=\beta/(\rho c_p)=1.51\ 10^{-7}\ m^2/s$ (thermal diffusivity) were taken for water at 37 °C.[22]

The choroidal blood flow, which was taken into account by a global perfusion term according to Eq. (15), has been measured by different groups.[17] For rabbits, the determined perfusion rate Q ranges from $Q=0.13\ s^{-1}$ (Ref. 36) to $Q=0.6\ s^{-1}$ (Ref. 37).

For the simulations, the temperature increase according to Eq. (15) was calculated for both absorbing layers separately. With respect to the linearity of the differential operators $\partial/\partial t$ and Δ [Eq. (10)], the principle of superposition can be applied, and the sum of both temperature increases results in the total increase T_{tot}:

$$T_{tot} = T_{rpe} + T_{chor}. \tag{16}$$

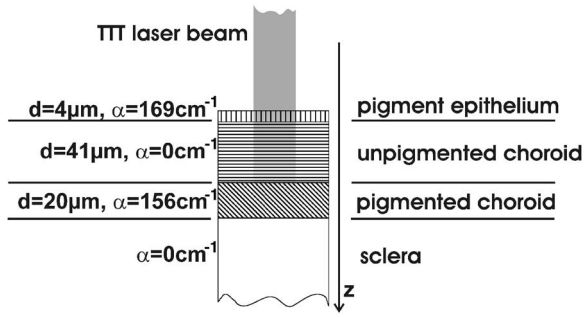

Fig. 4 Fundus geometry of a rabbit eye used for analytical modeling of temperature increase.[17]

3 Results

3.1 *Results from Analytical Modeling*

3.1.1 *Dorsal and lateral temperature profile*

In first analytical simulations, the lateral temperature increase during TTT laser irradiation was calculated for different depths in the fundus of the rabbit eye. A top-hat laser beam profile with a square length of $2a=2.66$ mm was assumed, which correlates to a circular spot diameter of 3 mm. The assumed power applied to the cornea was 300 mW, corresponding to 270 mW on the retina. According to Sec. 2.7, the overall absorption at the fundus is 31.6%. The calculated temperature increase at the end of the 60 s irradiation period over tissue depth and distance to the center of the spot is depicted in Fig. 5 in an isothermal diagram. For a better visualization, the layered structure of a rabbit eye is drawn on the right side of the graph according to Ref. 17, and the irradiation spot is drawn on top. Figures 6(a) and 6(b) depict a vertical and horizontal cross section in the center of the spot and along the surface of the RPE.

The results show that the calculated temperature increase after 60-s irradiation is 12.0 °C in the center of the spot on the RPE retina interface. The highest temperature increase of 12.2 °C is achieved in the choroid. Due to heat diffusion, the temperature in the vitreous decreases with an average gradient of about 1 °C/100 μm. For the lateral temperature profile, ΔT decreases as the distance to the center of the spot increases. The increase in temperature at the border of the spot is 36.3% less than in the center.

3.1.2 *Influence of pigmentation on the chorioretinal temperature increase*

One factor in chorioretinal temperature increase is its absorption. An especially important factor, which varies intra- and interindividual, is the density of the melanin in the RPE layer. Therefore, the temperature increase was calculated for different RPE absorption coefficients. Besides, the value used in the previous simulation with $\alpha_{rpe}=169\ cm^{-1}$, an RPE absorption of $\alpha_{rpe}=84.5\ cm^{-1}$ and $\alpha_{rpe}=253.5\ cm^{-1}$ was assumed. The total absorptions at the fundi are thus 29.2, 31.6, and 33.9% for $\alpha_{rpe}=84.5$, 169, and 253.5 cm^{-1}, respectively. The tem-

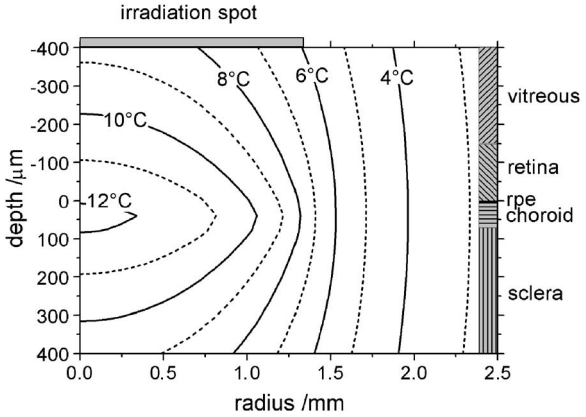

Fig. 5 Calculated temperature increase after 60-s heating with $a=1.33$ mm and $P=270$ mW on the retina without perfusion.

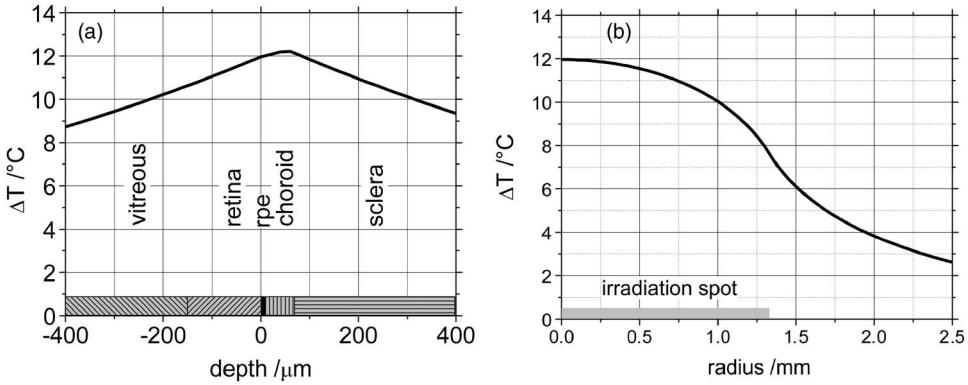

Fig. 6 (a) Calculated dorsal and (b) lateral temperature increase at the fundus of a rabbit eye after 60-s TTT laser irradiation with $a=1.33$ mm and $P=270$ mW on the retina without perfusion.

perature versus time is depicted in Fig. 7 for $x=y=z=0$, assuming the same laser parameters as in Sec. 3.1.1.

As expected, the course of the three curves is the same except for a constant factor. The maximum calculated temperature increase after 60-s irradiation is 7.8% less in the weakly pigmented than in the medium pigmented one. At the same time, it is 7.5% higher in the heavily pigmented RPE.

3.1.3 *Influence of perfusion on the chorioretinal temperature increase*

In a further simulation, the influence of perfusion on the retinal temperature increase was calculated. In Fig. 8(a), the calculated temperature increase over time is shown. The assumed laser parameters are the same as in Sec. 3.1.1. In contrast to the temperature curve without perfusion, the calculated temperature increase with heat convection reaches a constant temperature during irradiation time. At thermal equilibrium, the heat induced by the laser irradiation is equal to the energy leaving the area by heat conduction and blood flow. Figure 8(b) depicts the influence of the perfusion rate to the maximum temperature increase after a 60-s irradiation. As shown, the final temperature increase does not linearly decrease with the perfusion rate. With a perfusion rate of $Q=0.13$ s^{-1} (according to Ref. 36), the maximum temperature rise $\Delta T=7.4$ °C is 38.5% lower compared to the value $\Delta T=12.0$ °C obtained without perfusion. An even higher drop of 65.1% is seen for the maximum perfusion rate of 0.6 s^{-1} reported in Ref. 37.

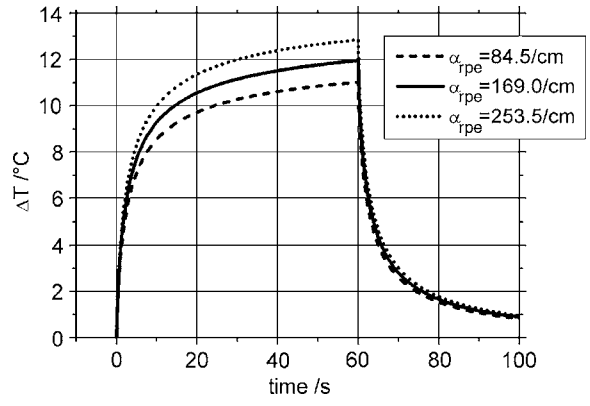

Fig. 7 Influence of different RPE absorptions on the retinal temperature increase with $a=1.33$ mm and $P=270$ mW on the retina.

In Fig. 8(c), the lateral temperature profiles after 60-s irradiation for different perfusion rates are depicted. Due to the perfusion, the temperature within the spot is more constant with an increasing temperature gradient to the border of the spot.

Another simulation concerns the ratio of temperature increase induced in the center of the laser spot ($x=y=0$) to the border ($x=a$, $y=0$). The result is shown in Fig. 8(d). Without perfusion, the calculated temperature ratio between the center and border is 1.57. The ratio increases with increasing perfusion up to a factor of 1.98 for a perfusion rate of 1.0.

3.2 *Determination of the Temperature-Dependent Tissue Parameters*

The maximal amplitude of the pressure wave in dependence of the temperature of retinal explants was measured for 12 porcine and two rabbit retinal explants. The explants were dissected from the globes and positioned in a cuvette. The cuvette was then filled with saline solution of 55 °C temperature.

Afterward, the radiation of the probe laser was applied to the explant. Within 30 min, the water bath was cooled down to 15 °C. During that time, about 100 data points were gained, with every data point being an average value of 30 pressure maxima for the same RPE temperature. Every measured maximal pressure was normalized to the corresponding pulse energy, thus compensating for pulse-to-pulse energy deviations of the laser source according to Eq. (3). The curves observed for the different retinal explants were normalized to a temperature of 37 °C and averaged. The standard deviation is less than 3% for all data points between 20 and 50 °C.

According to Eq. (7), a second-order polynomial was fitted to the averaged data. In Fig. 9, the temperature dependence of the detected pressure maximum for rabbit and porcine retinal explants is depicted. The graph shows averaged curves for 12 porcine and two rabbit eyes. For the fitting parameters T_0 and T_{max}, values of (-20.5 ± 1.1) °C and (114.4 ± 7.8) °C were obtained for the porcine RPE explants. The constants for rabbit RPE explants are $T_0=(-22.5\pm1.3)$ °C and $T_{max}=(150.4\pm17.3)$ °C, with the uncertainty being the error of

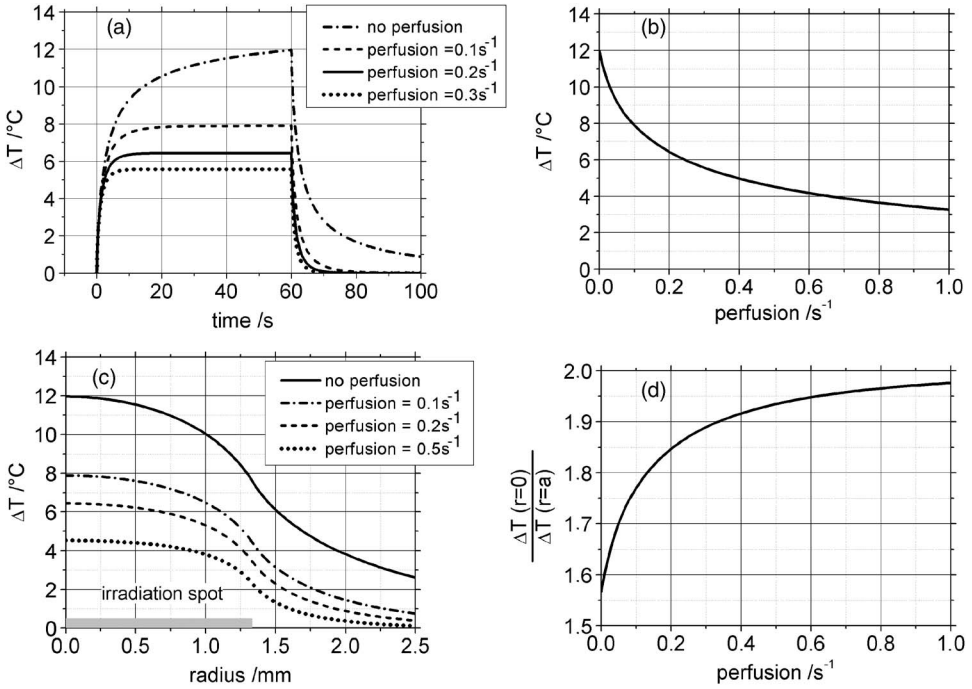

Fig. 8 Influence of perfusion on the temperature increase at the RPE surface with $a=1.33$ mm and $P=270$ mW on the retina. (a) Temperature increase over irradiation time. (b) Maximum temperature after 60 s of irradiation over perfusion rate. (c) Lateral temperature increase for different perfusion rates. (d) Ratio of ΔT in the center to the border of the spot versus perfusion rate.

the parameter value obtained by the non-linear curve fit. From 37 to 50 °C, the pressure maximum increases by 15.1% (pig) and 16.5% (rabbit).

The insert in Fig. 9 depicts a typical pressure transient as detected by the ultrasonic transducer. The observed oscillation of the signal shows the response function of the transducer.

In all of the following experiments, the average values of T_0 and T_{max} were used for calculations of the chorioretinal temperature increases using Eq. (8).

3.3 *Temperature Determination on Porcine Eyes (Ex Vivo)*

The chorioretinal temperature increase during TTT was determined by OA as well as by a thermocouple (TC) inserted transsclerally below the RPE layer for a quantification of the measurement accuracy. For the OA temperature determination, a retinal spot diameter of 0.3 mm and a pulse energy of 5 μJ was used. The retinal diameter of the TTT laser spot was 2 mm. The irradiation was increased in four steps. With consideration of 6% reflectance of the Mainster Standard contact lens, and the assumption of 16% absorption in the anterior ocular media as measured for human eyes,[32] retinal irradiances between 1.01 and 3.36 W/cm^2 were applied. The position of the eye, the probe laser spot, and the TTT laser spot were kept stable between the measurements. To obtain the individually different scaling factor s, 20 probe pulses were applied before each measurement and the average pressure maximum was detected at known ambient temperatures. The induced temperature increase during TTT laser irradiation over time is plotted in Fig. 10. Figure 10(a) shows the thermocouple measurement for the four different irradiations, while Fig. 10(b) depicts the corresponding OA determined temperatures. The deviation of the temperature courses is shown in Fig. 10(c).

The TTT laser was switched on 10 s after the OA measurement started and lasted for 60 s. Right after the irradiation started, the temperature steeply increased with a maximum temperature at the end of the irradiation. In Table 1, the maximum temperature increases at the end of the irradiation in dependence on the irradiance I for TC measurement and OA determination are shown. For all curves, the OA determination shows a slightly higher temperature increase than the direct measurement. The maximum temperature increases are 5.5 °C/(W/cm^2) measured by the TC, and 5.8 °C/(W/cm^2)

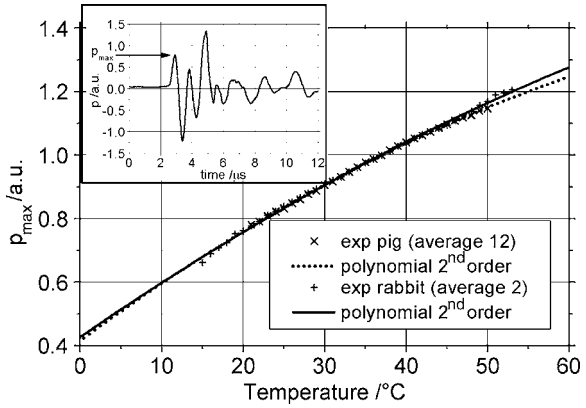

Fig. 9 Temperature dependence of maximum detected ultrasonic pressure signal for porcine and rabbit RPE explants and typical pressure transient as detected by the ultrasonic transducer.

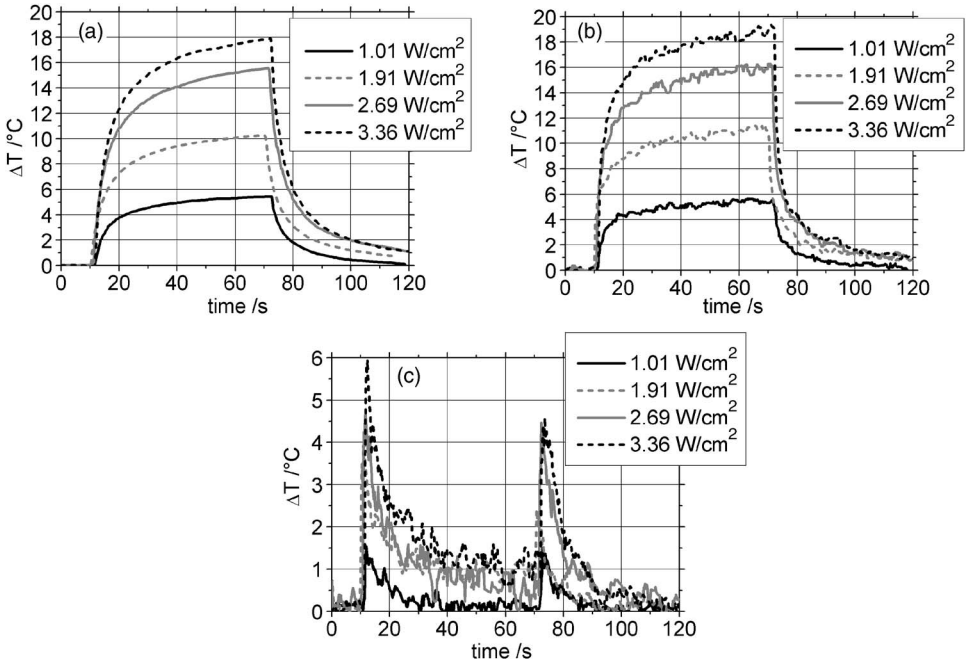

Fig. 10 Temperature increase during TTT on a porcine eye (*ex vivo*) (d=2 mm). (a) TC measurement; (b) OA determination; and (c) deviation of (a) and (b).

derived from OA determination. In Table 1, the deviation of ΔT_{max} is given in absolute values, and relative to the TC measurement. The maximum deviation is hereby up to 1.2 °C with a highest percentage deviation of 8.6%.

As shown in Fig. 10(c), the deviation varies with the irradiation time. The highest deviations occur at the beginning and right after the irradiation, caused by high differences in the slopes. The maximum temperature deviations are given in Table 1. The last column in Table 1 represents the average deviation for the irradiation time of 60 s.

The maximum deviation increases with the irradiance. The highest temperature deviation of 6.0 °C was observed for an irradiance of 3.36 W/cm^2 right after the TTT laser was switched on. The highest average temperature deviation of 1.7 °C was also derived for the same irradiance.

3.4 *Temperature Determination on Rabbit Eyes (In Vivo)*

Our first *in vivo* experiment served to investigate the correspondence and accuracy between OA and TC temperature determination on rabbits. Therefore, a miniaturized TC was inserted through a sclerotomy 1 mm posterior to the corneal limbus in the rabbit's eye. The tip of the TC was positioned into the center of the TTT laser spot into the subretinal space resting on top of the RPE.

Figure 11 shows a photograph of the rabbit fundus taken during TTT irradiation through the ocular of the slit lamp. The TC and its central position can clearly be seen. During the irradiation the TC was handheld.

For the experiment, a retinal spot diameter of 2 mm with a power of 129 mW measured in front of the contact lens was used for heating. Due to a reflectance of 2.8% in the Haag-Streit contact lens for 810-nm wavelength and assuming an absorption of 10% in the globe,[33,34] the retinal irradiance was 3.59 W/cm^2.

For the probe laser, a pulse energy of 6.3 μJ was used at a retinal spot diameter of 0.3 mm. Five measurements were performed consecutively with neither moving the laser spot nor changing the laser settings. Three temperature curves

Table 1 Maximum temperature increases for different irradiations on porcine eyes for TC measurement, and optoacoustic determination and deviation between the two measurement techniques.

I [W/cm^2]	ΔT_{max} tc [°C]	ΔT_{max} oa [°C]	ΔT_{max} dev [°C]	ΔT_{max} dev [%]	max dev [°C]	average dev [°C]
1.01	5.4	5.4	0	0	1.5	0.3
1.91	10.5	11.4	0.9	8.6	3.9	1.3
2.69	15.6	16.2	0.6	3.8	4.7	1.1
3.36	17.9	19.1	1.2	6.7	6.0	1.7

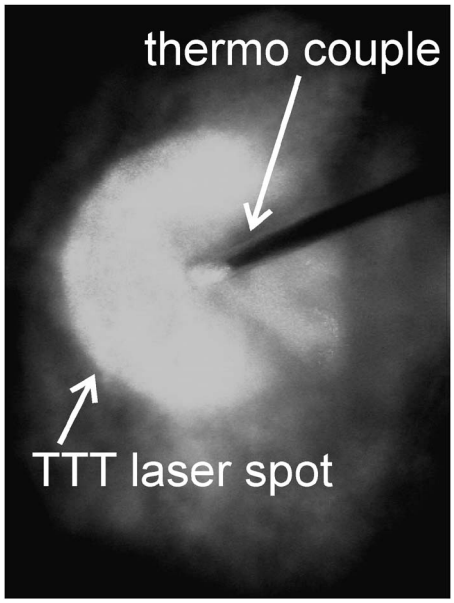

Fig. 11 Photograph of a rabbit fundus during TTT with a TC positioned in the center of the laser spot.

were determined by OA and two by means of the handheld TC, as depicted in Fig. 12.

As expected from temperature calculation [Fig. 8(a)], a constant temperature plateau within the irradiation time was achieved due to perfusion. In the described experiment, this plateau was reached 20 s after starting the TTT laser irradiation. The obtained plateau temperature measured by the TC is between 4.1 and 6.2 °C. The temperature data as determined by OA are mainly within the TC range.

For a comparison with analytical data, a calculated temperature curve was fitted to the experimental data assuming a fundus geometry and absorption coefficients as described in Sec. 2.7. The best accordance to the averaged experimental curves with a maximum temperature increase of 5.5 °C was achieved with a global perfusion rate of 0.13 s^{-1}.

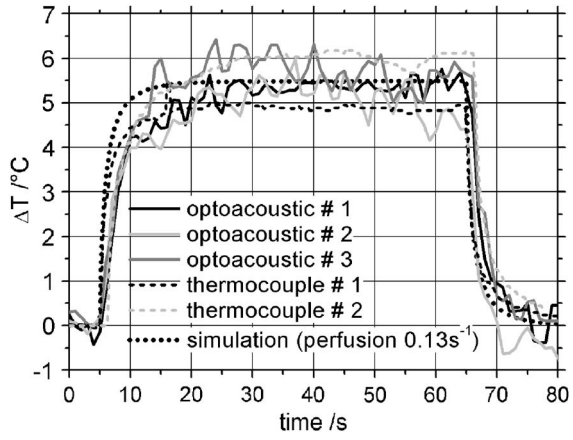

Fig. 12 Temperature increase at the fundus of a rabbit eye during TTT (*in vivo*). OA and TC measurement and calculated data are shown. (d=2 mm, I=3.59 W/cm^2).

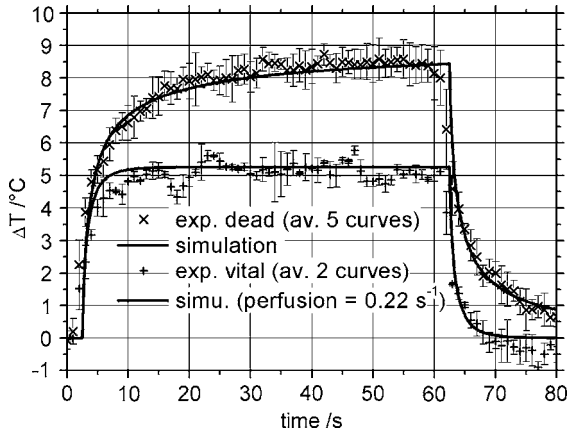

Fig. 13 Temperature increase at the fundus of a rabbit eye during TTT (*in vivo*), influence of perfusion (d=2 mm, I=3.9 W/cm^2).

The same rabbit was used for another experiment to quantify the influence of perfusion on the chorioretinal temperature increase during TTT. The temperature increase was determined by OA at the same area pre- and postmortem while keeping the position of the rabbit stable. The retinal irradiation was set to 3.90 W/cm^2 with a spot diameter of 2 mm. The probe laser parameters are the same as in the previous experiment. The rabbit underwent two irradiations *in vivo* and five postmortem. The averaged curves are plotted in Fig. 13. The error bars indicate the standard deviation of the averaged measurements.

In contrast to the living rabbit, the ΔT postmortem rose over the 60 s of irradiation. The averaged maximum temperature increase without perfusion was 8.6 °C compared to 5.3 °C with perfusion. Thus, ΔT_{max} increased by 62.2% postmortem.

The average standard deviation for the temperature increase with perfusion (two measurements) was 0.24 °C, whereas for the determination without perfusion a value of 0.47 °C was obtained.

The temperature slopes were calculated analytically. For the vital rabbit, a perfusion rate of 0.22 s^{-1} shows the best correspondence to experimental data. The results of the calculation are also plotted in Fig. 13. Both simulations for the vital and dead rabbit are in good accordance to the experimental gained data, with an average deviation during irradiation of 0.30 °C respective of 0.24 °C compared to the averaged experimental data.

In a further experiment, another rabbit underwent five TTT irradiations using slightly differing intensities on different retinal areas. For all irradiations, the temperature increase was determined by OA. Before the irradiation, the retina was marked by high intensity radiation of a diode laser coupled into an indirect ophthalmoscope with a retinal spot diameter of 0.5 mm. The distance between the rectangularly arranged spots was 5 mm in each direction. This marking was necessary for a better identification of the treated areas in fundus images.

The power of the TTT laser ranged from 115 to 148 mW. Due to a reflectance of the Mainster Standard contact lens of 6% and a retinal spot diameter of 2 mm, retinal irradiances between 3.10 and 3.96 W/cm^2 were achieved. The retinal

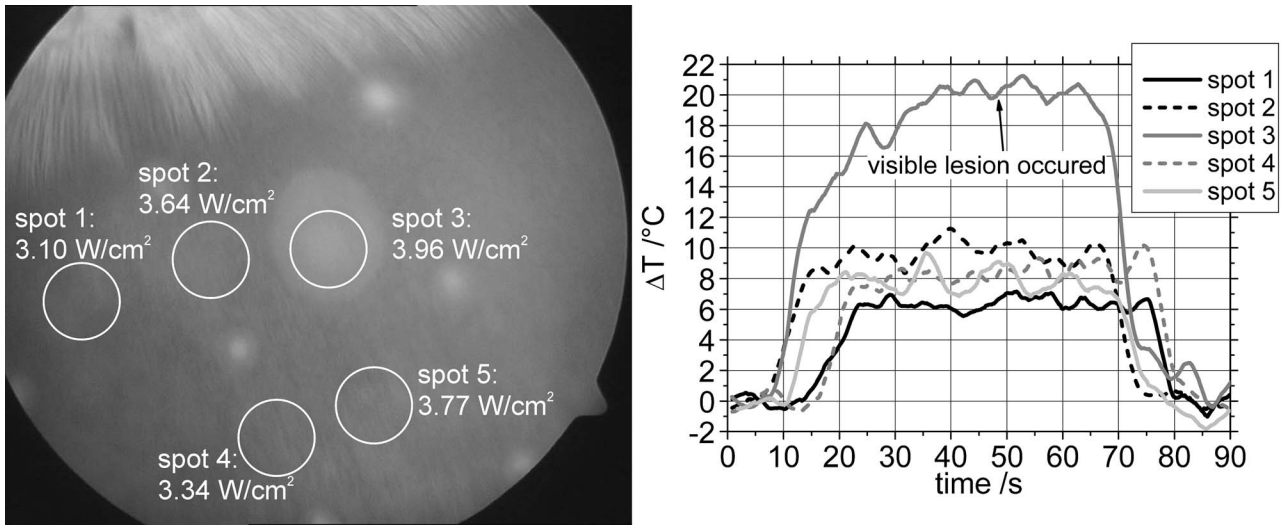

Fig. 14 (a) White light fundus image of rabbit eye after laser irradiation. The white spots are coagulations caused by the diode laser radiation. (b) Corresponding temperature increases (d=2 mm).

diameter of the probe laser spot was 0.3 mm with a pulse energy of 6.3 μJ. Figure 14 shows a fundus image of the rabbit eye after the laser irradiations. The five treated areas are marked by white circles, with the spot numbers in chronological order. The whole experiment took 30 min with at least five minutes between two irradiations. In the third irradiation (spot 3), a whitening of the retina occurred after 40 s of irradiation time.

The corresponding temperature slopes over time are plotted in Fig. 14(b). It is shown that for irradiations 1, 2, 4, and 5 with irradiances between 3.10 and 3.77 W/cm^2, an almost constant temperature increase was reached after 10-s irradiation time. The temperature increases for the plateaus are between 6.4 and 9.7 °C, while the temperature level is not linear in comparison to the individual irradiation. For the third irradiation with 3.96 W/cm^2, an extraordinary high temperature increase of more than 20 °C was obtained, even though the irradiation was only 5.0% higher than irradiation 5. The moment the lesion became visible to the ophthalmologist during the irradiation is demarcated with an arrow.

4 Discussion

It was demonstrated that the retinal temperature increase during laser irradiation can be optoacoustically determined noninvasively. The results are in agreement to TC measurements and fit very well with calculated data from temperature simulations. Moreover, the influence of different tissue parameters on the temperature increase can be quantified by using appropriate thermal model calculations.

In the following sections, the results are discussed in general and in detail considering a clinical application of this method for TTT.

4.1 *Analytical Modeling*

As many laser therapies in ophthalmology evoke a therapeutic effect due to heating, several temperature calculations have been performed, particularly models for laser photocoagulation at the retina with exposure times up to 300 ms.[16,17,24,38] However, the calculated temperatures are not linearly transferable to long exposure times like in TTT, since the perfusion in the choroid cannot be neglected for exposure times of seconds to minutes.

In the analytical model used for this work, the results should be understood as adjuvant for a general understanding of the temperature increases during laser irradiation of the fundus and the influence of the different tissue properties on it. The temperature increase and temporal course depend on the absorption of the different layers, their thickness and distances, as well as on the blood perfusion for long irradiation times as in TTT. The different influences are discussed in the following sections.

For exposure times of 60 s, the lateral temperature decreases as the radial distance to the center of the spot increases, as shown in Fig. 6(b). For a treatment, this fact should be accounted for by using spot diameters larger than the diseased area to obtain a sufficient temperature increase over the whole diseased area. However, the temperature difference between center and border of the spot might result in a central coagulation without having any effect to the outer area. To achieve a constant temperature profile over the whole irradiated area, it is necessary to change the lateral laser spot profile in such a way that the intensity is increasing with the distance to the center, e.g., by a ring profile or torus (doughnut mode).

The simulations on the dorsal temperature profile after 60 s of TTT irradiation show that the temperature within the absorbing layers of the eye is almost constant due to heat convection and the long exposure time. The long exposure time is also the reason why the total absorption of the fundus is of much higher interest for the temperature increase than the detailed absorption of RPE and choroid. By convection, the induced heat disperses over all fundus layers. The longer the exposure time, the smaller the influence of location and thickness of every absorbing layer, i.e., the influence of RPE pigmentation plays a minor role for this wavelength. The RPE absorption in the rabbit (6.54% for λ=810 nm) compared to

the choroidal absorption (26.80% for $\lambda = 810$ nm) is rather low. With increasing absorption ratio, the differences in RPE pigmentation might have a stronger influence on the temperature increase.

For shorter exposure times (e.g., photocoagulation with $\tau \approx 100$ ms), the RPE pigmentation has a much higher influence. For humans the calculated contribution to the total temperature increase from RPE layer is 65% compared to a choroidal contribution of 35%.[24] In this case, individually varied RPE pigmentation might result in high temperature differences.

Even though choroidal perfusion has a negligible effect in retinal photocoagulation,[39] the influence on the chorioretinal temperature increase during TTT was clearly shown. Even with a comparatively small perfusion rate of $0.1\ s^{-1}$, the maximum ΔT is 33.9% less than without perfusion. This might have a significant influence on TTT, because areas of high temperature might occur within the irradiated area, in which the individual perfusion is low. On the other hand, the temperature increase induced on areas above the main vessels might be obviously less than in surrounding areas.

The simulations that monitored the influence of perfusion on the temperature course [Fig. 8(c)] and the ratio of temperature increase induced between the center and the border of the spot [Fig. 8(d)] indicates that the temperature gradients at the border of the laser spot increase with perfusion. Increasing perfusion averages the temperature profile within the irradiated area with a rather steep gradient at the rim of the spot. In perfused tissue, the heated area is more localized within the spot, even though the maximum temperature is less.

In a medical application, the perfusion rate also depends on the intraocular pressure, which can be varied by the pressure of the contact lens to the cornea. Therefore, a higher pressure might result in reduced perfusion and thus induce a higher temperature increase during laser irradiation.

Overall, the utilized analytical model is adequate for a general understanding of the influence of tissue parameters on the shape and slope of the laser-induced temperature increase.

The main limitation is given by the assumption of a global perfusion rate, as the rabbit's physiology differs from this assumption. A thermal model with perfusion localized only in the choroid might result in much higher perfusion rates and different temperature slopes. Moreover, the assumption of a constant perfusion rate, independent of the observed area, does not reflect a retinal laser treatment very well, since for large spot sizes the blood will already accumulate heat as it crosses the irradiated spot. Such considerations cannot be implemented by analytical modeling and will be part of a numerical temperature model currently under development.

When observing a central temperature increase, the influence of a rectangular spot instead of a circular profile will have a minor influence, since the central heating induced by the border of the spot is comparably small. This is no longer valid if the temperature increase at the border shall be considered.

For large spot diameters, as given in TTT, the assumption of neglected scattering is appropriate, because most of the scattered light is absorbed within the irradiated area anyway, especially if a temperature increase in the center of the spot is regarded.

The influence of tissue heterogeneities like single melanosomes within the RPE is negligible for long irradiation times, as the heat conduction leads to an almost constant depth temperature profile during heating time. However, the results obtained in simulations are appropriate to generally describe temperature courses at the fundus. For a more realistic examination, a numerical model considering local perfusion in the choroid and a circular irradiation is needed. The implementation of such models is in progress.

4.2 *Temperature Dependence of the Grüneisen Parameter* Γ

The temperature dependence of the pressure wave maximum for porcine and rabbit retinal explants show an analog course in the measured temperature range. The findings for porcine retinal explants are similar to results obtained by Schüle et al. in related experiments, using a wavelength of 527 nm and a pulse length of 1.7 μs with a linear approximation, who obtained an increase in p_{max} of 14.6% from 37 to 50 °C.[14] The increase of p_{max} for water in the same range is with 30% about twice as large as for an eye fundus.[19]

In order to receive an adequate signal-to-noise ratio for every single pressure transient, it is desirable to obtain the highest possible pressure amplitude. It is therefore beneficial that the specimen shows a high absorption for the used laser wavelength. Due to the absorption curve for melanin,[31] the main absorber in the RPE, a maximum amplitude can be achieved using a wavelength in the visible range. The shorter the wavelength, the higher the absorption. The second important factor is the pulse duration. For a pulse duration longer than the acoustic transit time ($t_{trans} = 2.7$ ns for rabbit RPE with $d = 4$ μm), the induced pressure amplitude decreases almost exponentially with the pulse duration.[18] With respect to these two factors, the choice of a 500-nm wavelength with a pulse duration of 3.5 ns is adequate.

4.3 *Temperature Determination on Ex Vivo Eye Globes*

A general comparison between OA temperature determination and TC measurement on porcine eye globes shows a very good accordance.

As for TTT, the maximum temperature increase might cause the highest retinal damage; the measurement accuracy given by the deviation of ΔT_{max} between TC measurement and OA determination is important for the applicability of this technique. The deviation between TC measurement and OA temperature determination is comparatively small at the end of the irradiation compared to the beginning. The OA determination shows a much higher temperature gradient at the beginning. This might indicate that the position of the TC is too deep in the eye, resulting in a slower temperature increase. Another fact is that the spherical tip of the thermocouple with a diameter of 250 μm detects an average temperature of the tissue integrated over the contacted area. With increasing irradiation time, the difference is decreasing because the whole tissue is heated up with only marginal temperature differences resulting from depth (see Sec. 3.1.1).

The induced temperature increases proportionally to the applied laser power. The calculated temperature after a 60-s

irradiation is 5.5 °C/(W/cm^2) derived from the TC measurement and 5.8 °C/(W/cm^2) derived from OA determination.

The temperature curves for the OA determination are much noisier than the according TC measurements. Possible reasons are that the cable from the transducer to amplifier might act as an antenna inducing noise, which is thereafter also amplified by 54 dB, as well the noise of the amplifier itself.

4.4 *Temperature Determination and Simulation In Vivo*

Comparable OA temperature determination and TC measurement on a living rabbit show on one animal that the OA temperature determination is within the two temperature curves gathered by a thermocouple. As the thermocouple was handheld during the measurement, a precise positioning in the center and on the RPE without evoking lesions or retinal bleedings over the whole irradiation time is almost impossible. Even though the direct absorption of radiation of the thermocouple is negligible, the insertion from the same direction as the laser radiation causes differences in the heating process due to reflecting the radiation and causing shadowing on the fundus.

Compared to the *ex vivo* experiments on porcine eyes, the noise on the temperature data in rabbits is higher. The main reason is that the amplitude of the induced pressure wave is less due to a weaker absorption of the probe laser pulse in the rabbit's fundus. Another reason is a poorer acoustic adaption of the ultrasonic transducer to the cornea. The contact lens is designed for the radius of a human cornea, having the same radius as porcine cornea. Rabbit's corneal radii are smaller, resulting in poorer matching to the contact lens.

The calculated temperature increase for this experiment shows good correspondence to the average obtained experimental data by assuming a global perfusion rate of 0.13 s^{-1}. This is a realistic value for rabbit choroidal blood flow.[17] In further simulations, the assumed global perfusion rate needs to be reduced to a choroidal perfusion for a better comparison to literature data.

The proposed influence of perfusion to the chorioretinal temperature increase during TTT is verified experimentally for the first time. The calculated temperature curves are in very good accordance to the experimentally gained data. In this *in vivo* experiment, the assumed global perfusion rate of 0.22 s^{-1} is higher than in the previous experiment (Fig. 12), even though the experiments were performed on the same rabbit. This might indicate that the probe laser spot was positioned on a higher perfused area like a main vessel.

In the last experiment on rabbits, the influence of intraindividual factors on the retinal temperature increase can clearly be observed. In contrast to the *ex vivo* experiment on porcine eyes, (Fig. 10), the temperature slopes obtained at different retinal areas are not linearly increasing with the intensity. The individual factors accounting for an individual temperature increase cannot be determined beforehand. The areas appeared equal without hints for higher or lower pigmentation or choroidal perfusion rates under white light examinations.

The slope of the temperature increase observed for irradiation 3 is more comparable to slopes determined in *ex vivo* experiments. This might indicate that the perfusion for this irradiated area was very weak, causing the high temperature increase. This leads subsequently to a coagulation, which became visible as a whitening of the retina. The quantified temperature threshold of 21 °C is comparable to results by Ip, Kroll, and Reichel,[40] who obtained coagulation necrosis above 60 °C retinal temperature within 0.5 to 1 s.

In clinical TTT, the online determined temperature increases could have predicted this lesion before occurrence. The laser power could have been lowered, or the laser could even have been switched off to prevent such damage.

4.5 *Implications on Transpupillary Thermotherapy*

It was shown that the presented OA technique is sufficient for a retinal temperature determination during cw-laser irradiation. The instantaneous temperature increase caused by the absorption of the laser pulse can be estimated by $\Delta T = \alpha H / \rho c_V$.[19] For a pulse energy of 5 μJ and a spot diameter of 0.3 mm, this leads to an ΔT of less than 3 °C, assuming an absorption coefficient of 1700 cm^{-1} as realistic for human RPE.[24] This temporary temperature increase does not contribute significantly to the baseline temperature, as it is negligible at the occurrence of the following pulse.

The developed technique is safe for the patient and might also be used as a temperature-based dosimetry control to prevent under- and especially overtreatment during TTT. Further, the technique can be used to evaluate if an optimum treatment temperature exists, in which a therapeutic effect is evoked while below the coagulation temperature. Due to prosperous results, the power of the TTT laser might be automatically feedback controlled by the temperature information gained from the OA determination. Within the measurement accuracy, it should be possible to achieve a constant temperature increase independent of the individual tissue parameters of the patient, thus leading to a customized TTT application.

5 Conclusion

An optoacoustic technique allowing for a noninvasive real-time retinal temperature determination during, e.g, TTT is presented. In model calculations, the general influence of perfusion, pigmentation, and the location within the laser spot on the temperature increase is analyzed and discussed.

The temperature dependency of the tissue's Grüneisen parameter is found to follow a second-order polynomial correlation for rabbit and porcine eyes. In *in vivo* experiments on rabbits, the influence of perfusion on laser-induced temperature increase is for the first time determined experimentally. After 60 s, the temperature increase observed on the area without perfusion is 62.2% higher than on the same spot with perfusion. A whitening of a rabbit's retina is observed at a temperature increase of about 20 °C after 40 s. With the knowledge of the temperature course and the occurrence of damage, the Arrhenius parameters could possibly be determined for the regarded tissue.

In conclusion, the presented optoacoustic technique might serve as an adequate tool for temperature-based dosimetry control during TTT.

Acknowledgments

This project was supported by grants from the German Ministry of Education and Research, BMBF (grant number

01EZ0311). The authors are grateful to the diploma students Carolin Hartert and Markus Hilmes for their experimental contributions to the project.

References

1. Macular Photocoagulation Study Group, "Laser photocoagulation of subfoveal recurrent neovascular lesions in age-related macular degeneration. Results of a randomized clinical trial," *Arch. Ophthalmol. (Chicago)* **109**(9), 1232–1241 (1991).
2. Treatment of Age-Related Macula Degeneration with Photodynamic Therapy Study Group, "Photodynamic therapy of subfoveal choroidal neovascularization in age-related macular degeneration with verteporfin: one-year results of 2 randomized clinical trials-TAP report," *Arch. Ophthalmol. (Chicago)* **117**(10), 1329–1345 (1999).
3. J. Roider, R. Brinkmann, and R. Birngruber, "Selective retinal pigment epithelium laser treatment–Theoretical and clinical aspects," *Lasers in Opthalmology–Basic, Diagnostic and Surgical Aspects*, edited by Fankhauser and Kwasniewska (Kugler, The Hague, 2003).
4. R. S. Newsom, J. C. McAlister, M. Saeed, and J. D. McHugh, "Transpupillary thermotherapy (TTT) for the treatment of choroidal neovascularisation," *Br. J. Ophthamol.* **85**(2), 173–178 (2001).
5. A. H. Rogers and E. Reichel, "Transpupillary thermotherapy of subfoveal occult choroidal neovascularization," *Curr. Opin. Ophthalmol.* **12**(3), 212–215 (2001).
6. A. Kumar, G. Prakash, and R. P. Singh, "Transpupillary thermotherapy for idiopathic subfoveal choroidal neovascularization," *Acta Ophthalmol. Scand.* **82**, 205–208 (2004).
7. M. A. Mainster and E. Reichel, "Transpupillary thermotherapy for age-related macular degeneration: long-pulse photocoagulation, apoptosis, and heat shock proteins," *Ophthalmic Surg. Lasers* **31**(5), 359–373 (2000).
8. R. S. Newsom, J. C. McAlister, M. Saeed, K. El-Ghonemy, and J. D. McHugh, "Results 28 months following transpupillary thermotherapy for classic and occult choroidal neovascularization in patients with age-related macular degeneration," *Ophthalmic Surg. Lasers* **36**(2), 94–102 (2005).
9. E. Reichel, A. M. Berrocal, M. Ip, A. J. Kroll, V. Desai, J. S. Duker, and C. A. Puliafito, "Transpupillary thermotherapy of occult subfoveal choroidal neovascularization in patients with age-related macular degeneration," *Ophthalmology* **106**(10), 1908–1914 (1999).
10. K. Larin, I. Larina, M. Motamedi, and R. Esenaliev, "Monitoring of temperature distribution in tissues with optoacoustic technique in real time," *Proc. SPIE* **3916**, 311–321 (2000).
11. R. O. Esenaliev, I. V. Larina, K. V. Larin, and M. Motamedi, "Real-time optoacoustic monitoring during thermotherapy," *Proc. SPIE* **3916**, 302–310 (2000).
12. R. O. Esenaliev, A. A. Oraevsky, K. V. Larin, I. V. Larina, and M. Motamedi, "Real-time optoacoustic monitoring of temperature in tissues," *Proc. SPIE* **3601**, 268–275 (1999).
13. G. Schüle, G. Hüttmann, J. Roider, C. Wirbelauer, R. Birngruber, and R. Brinkmann, "Optoacoustic measurements during μs-irradiation of the retinal pigment epithelium," *Proc. SPIE* **3914**, 230–236 (2000).
14. G. Schüle, G. Hüttmann, C. Framme, J. Roider, and R. Brinkmann, "Noninvasive optoacoustic temperature determination at the fundus of the eye during laser irradiation," *J. Biomed. Opt.* **9**(1), 173–179 (2004).
15. J. Kandulla, H. Elsner, M. Hilmes, C. Hartert, and R. Brinkmann, "Optoacoustic temperature determination at the fundus of the eye during transpupillary thermotherapy," *Proc. SPIE* **5688**, 208–214 (2005).
16. R. Birngruber, F. Hillenkamp, and V. P. Gabel, "Theoretical investigations of laser thermal retinal injury," *Health Phys.* **48**(6), 781–796 (1985).
17. R. Birngruber, "Choroidal circulation and heat convection at the fundus of the eye," in *Laser Applications in Medicine and Biology*, M. L. Wolbarsht, Ed., pp. 277–361, Plenum Press, New York (1991).
18. G. Paltauf and P. E. Dyer, "Photomechanical processes and effects in ablation," *Chem. Rev. (Washington, D.C.)* **103**, 487–518 (2003).
19. G. Paltauf and H. Schmidt Kloiber, "Microcavity dynamics during laser-induced spallation of liquids and gels," *Appl. Phys. A: Mater. Sci. Process.* **62**(4), 303–311 (1996).
20. V. E. Gusev and A. A. Karabutov, *Laser Optoacoustics*, American Institute of Physics, New York (1993).
21. M. W. Sigrist and F. K. Kneubühl, "Laser-generated stress waves in liquids," *J. Acoust. Soc. Am.* **64**(6), 1652–1663 (1978).
22. D. R. Lide, *Handbook of Chemistry and Physics*, CRC Press, Boca Raton, FL (1995).
23. V. P. Skripov, E. N. Sinitsyn, P. A. Pavlov, G. V. Ermakov, G. N. Muratov, N. V. Bulanov, and V. G. Baidakov, *Thermophysical Properties of Liquids in the Metastable (Superheated) State*, Gordon and Breach Science Publishers, New York (1988).
24. A. Vogel and R. Birngruber, "Temperature profiles in human retina and choroid during laser coagulation with different wavelengths ranging from 514 to 810 nm," *Lasers Light Ophthalmol.* **5**(1), 9–16 (1992).
25. A. J. Welch, "The thermal response of laser irradiated tissue," *IEEE J. Quantum Electron.* **20**(12), 1471–1480 (1984).
26. J. Roider and R. Birngruber, "Solution of the heat conduction equation," in *Optical-Thermal Response of Laser-Irradiated Tissue*, A. J. Welch and M. J. C. v. Gemert, Eds., pp. 385–409, Plenum Press, New York (1995).
27. D. E. Freund, R. L. McCally, R. A. Farrell, and D. H. Sliney, "A theoretical comparison of retinal temperature changes resulting from exposure to rectangular and Gaussian beams," *Lasers Life Sci.* **7**(2), 71–89 (1996).
28. D. E. Freund and D. H. Sliney, "Dependence of retinal model temperature calculations on beam shape and absorption coefficients," *Lasers Life Sci.* **8**, 229–247 (1999).
29. V. P. Gabel, "Die lichtabsorption am augenhintergrund," State Doctorate, Medizinische Fakultät, Ludwig Maximilians-Universität (1974).
30. V. P. Gabel, R. Birngruber, F. Hillenkamp, I. H. L. Wallow, and W. Schmolke, "Über die lichtabsorption am augenhintergrund," in *73. Zusammenkunft der Deutschen Ophthalm.*, Gesellschaft, Ed., pp. 362–367, J.F. Bergmann, München, Germany (1973).
31. V. P. Gabel, R. Birngruber, and F. Hillenkamp, "Visible and near infrared light absorption in pigment epithelium and choroid," in *XXIII Concilium Ophthalmologicum*, K. Shimuzu, Ed., pp. 658–662, Elsevier, Kyoto (1978).
32. E. Boettner and J. R. Wolter, "Transmission of the ocular media," *Invest. Ophthalmol.* **1**, 776–783 (1962).
33. P. V. Algvere, P. A. L. Torstensson, and B. M. Tengroth, "Light transmittance of ocular media in living rabbit eyes," *Invest. Ophthalmol. Visual Sci.* **34**(2), 349–354 (1993).
34. H. Wiesinger, F. H. Schmidt, R. C. Williams, C. O. Tiller, R. S. Ruffin, D. Guerry, and W. T. Ham, Jr., "The transmission of light; through the ocular media of the rabbit eye," *Am. J. Ophthalmol.* **42**(6), 907–910 (1956).
35. T. J. van den Berg and H. Spekreijse, "Near infrared light absorption in the human eye media," *Vision Res.* **37**(2), 249–253 (1997).
36. D. M. O'Day, M. B. Fish, S. B. Aronson, A. Coon, and M. Pollycove, "Ocular blood flow measurement by nuclide labeled microspheres," *Arch. Ophthalmol. (Chicago)* **86**(2), 205–209 (1971).
37. A. Bill, "Quantitative determination of uveal blood flow in rabbits," *Acta Physiol. Scand.* **55**, 101–110 (1962).
38. C. P. Cain and A. J. Welch, "Measured and predicted laser-induced temperature rises in the rabbit fundus," *Invest. Ophthalmol.* **13**(1), 60–70 (1974).
39. R. Birngruber, W. Weinberg, V. P. Gabel, and H. Kain, "Der Einfluss der Aderhautdurchblutung auf die Entstehung von Thermischen Läsionen am Augenhintergrund," in *Chirurgie der Lider und Tränenwege*, W. Jaeger Ed., pp. 705–710 (J. F. Bergmann, 1980).
40. M. Ip, A. Kroll, and E. Reichel, "Transpupillary thermotherapy," *Semin Ophthalmol.* **14**(1), 11–18 (1999).